www.dergipark.gov.tr
ISSN:2148-3736
El-Cezerî Fen ve Mühendislik Dergisi
Cilt: 8, No: 3, 2021 (1495-1510)

El-Cezerî Journal of Science and Engineering
Vol: 8, No: 3, 2021 (1495-1510)
DOI :10.31202/ecjse.951527

ECJSE

Research Paper / Makale

Synthesis, Characterization, and Theoretical Inhibitor Study for (1E,1'E)-2,2'-thiobis(1-(3-mesityl-3-methylcyclobutyl)ethan-1-one) Dioxime

Pelin KOPARIR[a], Rebaz Anwar OMER[b*], Arzu KARATEPE[c], Lana Omer AHMED[d]

[a]Institute of Forensics, Department of Chemistry, Malatya, TURKEY
[b]Department of Chemistry, Faculty of Science & Health, Koya University, Koya KOY45, F.R.Iraq
[b,c]Department of Chemistry, Faculty of Science, Firat University, 23169, Elazig, TURKEY
[d]Department of Physics, Faculty of Science & Health, Koya University, Koya KOY45, F.R. Iraq
[d]Department of Physics, Faculty of Science, Firat University, 23169, Elazig, TURKEY
rebaz.anwar@koyauniversity.org

Received/Geliş: 12.06.2021 **Accepted/Kabul:** 28.07.2021

Abstract: In this study synthesized and characterization of (1E,1'E)-2,2'-thiobis(1-(3-mesityl-3-methylcyclobutyl)ethan-1-one) dioxime for both experimental and computational was reported. The solid-state FT-IR spectrum was observed in the range of 4000–400 cm^{-1} and CDCl3 solvents were used for ^{1}H and ^{13}C NMR analysis. The molecular geometry was calculated using the Density Functional Theory (DFT/B3LYP) method in the ground state with the 6-31G(d, p) basis sets. Vibrational assignments and chemical shifts have been measured theoretically and compared to experimental data. B3LYP/6-31G(d,p) applied on our title compound to found different parameters such as the energy of the highest occupied molecular orbital (E_{HOMO}), the energy of the lowest unoccupied molecular orbital (E_{LUMO}), energy gap ($\Delta E = E_{LUMO} - E_{HOMO}$) and the dipole moment (μ) related to the corrosion efficacy of organic compounds whose molecular geometry and electronic properties are especially studied were calculated. Properties such as hardness (η), softness (σ), electronegativity (χ) values were computed using these measurement results to inhibitor activity. The fraction of transferred electrons (ΔN) was also calculated, which determined the interaction between the iron surface and the organic compounds. Corrosion inhibitor behavior can therefore be predicted without an experimental study. The findings of the calculations show good relation between organic-based corrosion inhibitors and quantum chemical parameters process.

Keywords: Dioxime, Experimental Spectroscopy, Theoretical spectroscopy, DFT, Inhibitor activity

(1E,1'E)-2,2'-tiobis(1-(3-mesitil-3-metilsiklobutil)etan-1-on) Dioksim için Sentez, Karakterizasyon ve Teorik İnhibitör Çalışması

Öz: Bu çalışmada (1E,1'E)-2,2'-thiobis(1-(3-mesityl-3-methylcyclobutyl)ethan-1-one) dioxime sentezlenmiş ve hem deneysel hem de sayısal olarak karakterizasyonu rapor edilmiştir. Katı faz FT-IR spektrumu 4000–400 cm^{-1} aralığında gözlemlendi ve ^{1}H ve ^{13}C NMR analizi için $CDCl_3$ solventleri kullanıldı. Moleküler geometri, 6-31G(d, p) temel setleri ile temel durumda Yoğunluk Fonksiyonel Teorisi (DFT/B3LYP) yöntemi kullanılarak hesaplandı. Titreşim sinyalleri ve kimyasal kaymalar teorik olarak ölçülmüş ve deneysel verilerle karşılaştırılmıştır. Başlıktaki bileşiğimize uygulanan B3LYP/6-31G(d,p), en yüksek dolu moleküler orbitalin enerjisi (EHOMO), en düşük boş moleküler orbitalin enerjisi (E_{LUMO}), enerji boşluğu ($\Delta E = E_{LUMO} - E_{HOMO}$) ve özellikle moleküler geometrisi ve elektronik özellikleri çalışılan organik bileşiklerin korozyon etkinliğine ilişkin dipol momenti (μ) hesaplanmıştır. Bu ölçüm sonuçları kullanılarak inhibitör aktiviteye sertlik (η),

How to cite this article
Koparir, P., Omer, R.A., Karatepe A., Ahmed, L.O., "Synthesis, Characterization, and Theoretical Inhibitor Study for (1E,1'E)-2,2'-thiobis(1-(3-mesityl-3-methylcyclobutyl)ethan-1-one) Dioxime" El-Cezerî Journal of Science and Engineering, 2021, 8 (3); 1495-1510.

Bu makaleye atıf yapmak için
Koparir, P., Omer, R.A., Karatepe A., Ahmed, L.O. *"(1E,1'E)-2,2'-tiobis(1-(3-mesitil-3-metilsiklobutil)etan-1-on) Dioksim için Sentez, Karakterizasyon ve Teorik İnhibitör Çalışması"* El-Cezerî Fen ve Mühendislik Dergisi 2021, 8 (3); 1495-1510.
ORCID ID: [a]0000-0002-3981-9748, [b]0000-0002-3774-6071 , [c]0000-0003-2791-7890 , [d]0000-0003-2181-1972

yumuşaklık (σ), elektronegatiflik (χ) değerleri gibi özellikler hesaplanmıştır. Demir yüzeyi ile organik bileşikler arasındaki etkileşimi belirleyen transfer edilen elektronların oranı (ΔN) da hesaplandı. Korozyon önleyici davranışı bu nedenle deneysel bir çalışma olmadan tahmin edilebilir. Hesaplamaların bulguları, organik bazlı korozyon inhibitörleri ile kuantum kimyasal parametreler süreci arasında iyi bir ilişki olduğunu göstermektedir.

Anahtar Kelimeler: Dioksim, Deneysel Spektroskopi, Teorik spektroskopi, DFT, İnhibitör aktivitesi

1. Introduction

An oxime is a chemical compound that belongs to the imines family and has the general formula $R_1R_2C=NOH$, where R_1 is an organic side-chain and R_2 is either hydrogen or another organic group, forming an aldoxime or a ketoxime. The term oxime was invented in the nineteenth century and is derived from a mixture of the terms oxygen and imine.

Oximes have an amphoteric group (C=NOH), it comprises a moderately acidic hydroxyl group and a slightly simple nitrogen atom [1]. The aliphatic group of oximes is more resistant to hydrolysis than the equivalent hydrazones. In the infrared spectrum, oximes have three distinct bands with wavenumbers of 3600 (O-H), 945 (N-O), and 1665 (C=N) (refer to stretching vibrations) [2]. Oximes are becoming increasingly important as analytical, biochemical, antifungal, antibacterial, and antimicrobial reagents, as well as for their high capacity to remove heavy metals, and their use as dyes has attracted interest [3-7].

Oximes are widely used in science, pharmaceutical synthesis, and the large-scale processing of organic chemicals. The structural characteristics of coordination compounds, as well as the peculiar reactivity modes of oximes and their complexes, are studied in depth [8-11].

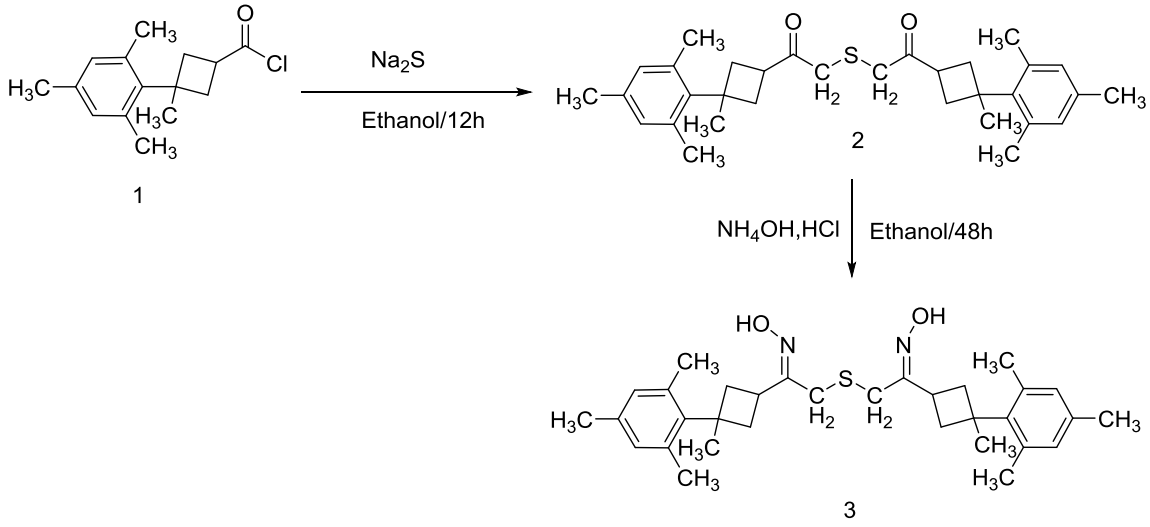

Figure 1. Steps for synthesized title compound.

Over the past ten years, the Density Functional Theory (DFT) has become the most common approach in computational chemistry. Provided molecular geometry, we determined the electronic structure and spectroscopic assignments of a molecule. DFT offers a range of methods, including LSDA, BPV86, and B3LYP. Becke 3-parameter Lee, Yang, and Parr correlation (B3LYP) density functional theory (DFT) [12-15]. Due to their consistent findings with experimental data in fields like physics, chemistry, and materials science, B3LYP has gained a lot of interest.

The title compound is first synthesized in our laboratories (Figure 1), and there is no knowledge about its molecular and vibrational spectroscopic properties in the previous literature. The synthesis, molecular structure, and spectroscopic characterization with the inhibitor activity of the title compound are all part of our research. A mix of experimental and theoretical research is used in this article. The FT-IR and NMR (^{1} H and ^{13}C) spectra were recorded. The optimized geometry of the synthesized compound was also determined theoretically. The experimental data was compared to the computed molecular structures (geometric parameters), theoretical scaled vibrational spectra (vibration frequencies), and NMR spectra (chemical shifts). Using Theoretical calculation to determine the anti-corrosion activity for title compound were study.

2. Experimental

All of the chemicals reagent grade and were used as-is, with no further purification. Gallenkamp melting point apparatus was used to determine the melting point. Using a Mattson 1000 FT-IR spectrometer and KBr pellets, the IR spectrum of the title compound was recorded in the range 4000–400 cm^{-1}. On a Varian-Mercury-Plus 200 MHz spectrometer, the ^{1}H and ^{13}C nuclear magnetic resonance (NMR) spectra were registered with CDCl-d6 as the solvent.

2.1 Synthesis and Characterization

2,2'-thiobis(1-(3-mesityl-3-methylcyclobutyl)ethan-1-one) (2)

In 100 ml round bottom flask 2.64 g (0.01 mol) 1-Mesitylene-1-Methyl-3- (2-Chlorine-1-Oxyethyl) Cyclobutane, 1.2 g (0.005 mol) $Na_2S.9H_2O$, 60 ml ethyl alcohol the reaction flask allocated with reflux for 12 hours at 55-60 ^{0}C. The precipitated was formed in hexane, dried and crystallized in ethyl alcohol. Yield 80%, M.p. 194 ^{0}C, IR (cm^{-1}): 3105 Cyclo alkane (υC-H); 3049 aromatic (υC-H); 2980-2870 aliphatic (υC-H); 1695 (υC=O); 1600- 1590 aromatic (υC=C); and 690-655 (υC-S-C). ^{1}H-NMR (200MHz, CDCl3, δ): 6.71 (s, 4H, Ar-H); 3.54-3.31 (m, 2x1H, cyclobutane; 2x2H, -CH2-S); 2.51-2.22 (m, 2x4H, Cyclobutane CH2); 2.16 (s, 2x9H, mesitylene CH3); 1.49 (s,2 x 3H, CH3 proton).^{13}C-NMR (200 MHz, CDCl3, ppm); The structure is symmetry. 207.97 (C=O); 145.09,136.23,135.66,131.79, (Aromatic C's); 42.24, 41.82, 4015, 26.46, (cyclobutane and aliphatic-CH2); 21.85 (CH3). Elemental Analysis Results; Theoretical / Experimental C: 78.32 / 78.24, H: 8.63 / 8.73, S: 6.53 / 6.49; $C_{32}H4_2O_2S$; M.wt: 490g/mol.

(1E,1'E)-2,2'-thiobis(1-(3-mesityl-3-methylcyclobutyl)ethan-1-one) dioxime (3)

In 100 ml round-bottom flask contain 4.9 g (0.01 mol) 2,2'-thiobis(1-(3-mesityl-3-methylcyclobutyl)ethan-1-one), 2.13 g (0.03 mol) hydroxylamine Hydrochloride and 1.2 g (0.03 mol) NaOH was prepared in 50 ml ethanol, the reaction flask allocated with reflux and thermometer was continued at 65-70Ċ for 2 days. It was precipitated in ice water, the precipitate was washed with water and dried in the open air, and crystallized in ethyl alcohol. M.p.:293 ^{0}C, yield %91. IR (cm^{-1}): 3348-3253 (υO-H); 3107 Cyclo alkane (υC-H); 3055 aromatic (υC-H); 2980-2870 aliphatic (υC-H); 1650-1600 (υC=N); 1600 aromatic (υC=C) and 690-655 (υC-S-C). ^{1}H-NMR (200MHz, CDCl3, δ): 10.66-10.63 (br, 2xH, N-OH); 6.71 (s,4H, Ar-H); 3.35-3.18 (m, 2x1H, cyclobutane; 2x2H, -CH2-S); 2.52-2.31 (m, 2x4H, cyclobutane CH2); 2.15 (s, 2x9H, mesitylene CH3); 1.48 (s,2 x 3H, CH3 proton). ^{13}C-NMR (200 MHz, CDCl3, ppm); 158.51 (C=N-OH); 145.74,136.24,135.47,131.79 (Aromatic C's); 43.25, 41.82, 40.15, 26.46, (cyclobutane and aliphatic-CH2); 21.85 (CH3). Elemental Analysis Results; Theoretical / Experimental C: 73.80/73.79, H: 8.52/8.53, N: 5.38/15.28, S: 6.16/6.92. $C_{32}H_{44}N_2O_{2S}$, M.wt: 520 g/mol.

3. Computational Characterization

The Gaussian 09 package was used to perform all of the calculations and the molecular visualization software Gauss-View, on a computer without any symmetry restrictions for the title compound [16, 17]. Density Functional Theory (DFT)/B3LYP using the basis sets 6-31G(d, p) were used to optimize the initial guess of the compound for a modeling structure. Geometric parameters (bond lengths, bond angles, torsion angles) of the title compound have been computed theoretically and compared with reference data based on the optimized geometry of the molecule. On the optimized molecule, the theoretical harmonic frequencies and chemical shifts were computed for the same levels in the ground state. B3LYP is also suited for workstation capability in the Gaussian09W program at 6-31G(d,p) basis set. The Identifiers of electronic structure from all geometry structures the energy of the highest occupied molecular orbital (E_{HOMO}), the energy of the lowest unoccupied molecular orbital (E_{LUMO}), energy bandgap ($\Delta E = E_{LUMO} - E_{HOMO}$), and the dipole moment (μ), hardness (η), softness (σ), electronegativity (χ), electrophilicity (ω) index, nucleophilicity (ε) index, chemical potential (Pi) and the fraction of transferred electrons (ΔN) related with corrosion inhibition activity were calculated.

4. Results and Discussion

4.1 Molecular Geometry

The molecular structure of the title compound was determined using the Density Functional Theory (DFT/B3LYP) method in the ground state with the 6-31G(d, p) basis sets. Figure 2. show molecular structures of (1E,1'E)-2,2'-thiobis(1-(3-mesityl-3-methylcyclobutyl) ethan-1-one) dioxime drawing by GAUSVIEW. Table 2 lists the optimized geometrical parameters (bond lengths, bond angles, and torsion angles) determined using B3LYP/6-31G(d,p) methods. Mesitylene, cyclobutane, and oxime groups make up our molecule's composition. For the cyclobutane ring in the compound, the average bond lengths between carbon atoms is 1.55 ^{0}A and the average bond angles formed by the three carbons is 109.25^0. There are no major variations between these values and those stated previously for cyclobutane derivatives [18-21]. The bond length between S-C is equal to 1.84 ^{0}A this value very close to the literature [22, 23]. The average bond length for the methyl group in a mesitylene group was equal to 1.51 ^{0}A. the mesitylene group is in the chair conformation the bond angle equal between carbon is 119.98 ^{0}A. The bond angle conformation is equal to 109.5, for our title compound, the angle obtained between S-C-C is equal to 109.87 ^{0}A. According to the results, the theoretical calculation was promised to found the best geometrical structure for the title compound.

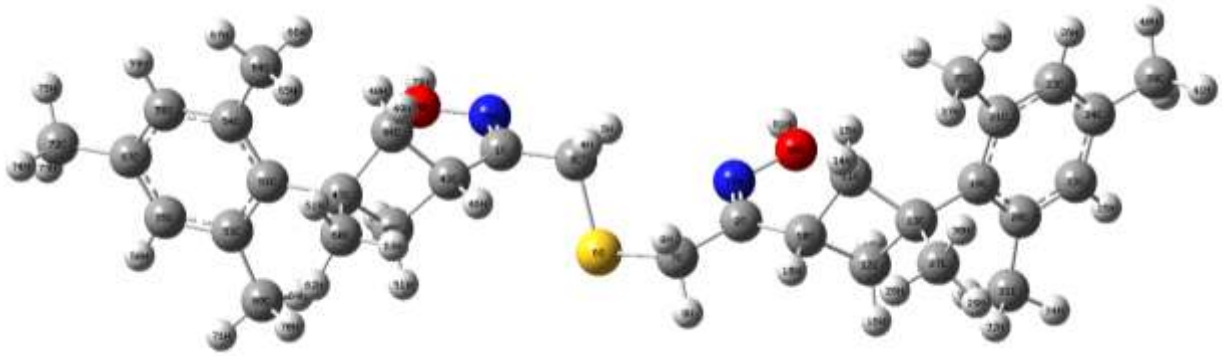

Figure 2. Geometrical structure of title compound

4.2 NMR Spectroscopy

The experimental Hydrogen (^{1}H) and carbon (^{13}C) chemical shifts for the title compound were investigated in chloroform ($CDCl_3$). Also in chloroform solvents, the theoretical ^{1}H and ^{13}C chemical shift values were determined using the DFT (B3LYP) method with the 6-31G (d, p) basis sets, all results were presents in Table 3 and 4.

Table 1. Bond Length, Bond angle and Dihedral angle for title compound.

Symbol	Bond Length	Symbol	Bond Angle	Symbol	Dihedral angle
C2-C5	4.9285437	C3-C5-C2	9.6608675	S4-C3-C5-C2	-14.9717739
C3-C5	1.5088024	S4-C3-C5	109.8769142	C5-C2-C5-C3	121.8768322
S4-C3	1.8496868	C5-C2-C5	51.9571056	C6-C2-C5-C3	56.2188812
C5-C2	1.5184349	C6-C2-C5	155.669436	C7-C6-C2-C5	-75.2691459
C6-C2	1.5101585	C7-C6-C2	121.2194727	C8-C6-C2-C5	177.1099023
C7-C6	1.5537011	C8-C6-C2	120.1442799	C9-C8-C6-C2	144.2423248
C8-C6	1.5539475	C9-C8-C6	89.6256166	C10-C9-C8-C6	-138.8904259
C9-C8	1.5722395	C10-C9-C8	118.0176977	C11-C10-C9-C8	-40.5665608
C10-C9	1.5344736	C11-C10-C9	121.0175218	C12-C10-C9-C8	142.7696268
C11-C10	1.4173368	C12-C10-C9	120.9770134	C13-C11-C10-C9	178.9397094
C12-C10	1.4175165	C13-C11-C10	119.8959816	C14-C12-C10-C9	-178.9826215
C13-C11	1.4001342	C14-C12-C10	119.9361287	C15-C13-C11-C10	1.3911537
C14-C12	1.3999982	C15-C13-C11	122.5114568	C16-C9-C8-C6	92.8163165
C15-C13	1.3935274	C16-C9-C8	111.2419658	C17-C11-C10-C9	-2.248742
C16-C9	1.5421268	C17-C11-C10	123.7235199	C18-C12-C10-C9	2.1600067
C17-C11	1.5176296	C18-C12-C10	123.6477953	C19-C15-C13-C11	179.0019222
C18-C12	1.5174423	C19-C15-C13	121.4153998	C20-C1-C3-C4	69.0800191
C19-C15	1.5103808	C20-C1-C3	118.6372296	C21-C20-C1-C3	127.1055761
C20-C1	1.5074314	C21-C20-C1	120.7269945	C22-C20-C1-C3	-125.4149789
C21-C20	1.554353	C22-C20-C1	120.5354565	C23-C21-C20-C1	143.7488175
C22-C20	1.5525955	C23-C21-C20	89.5735673	C24-C23-C21-C20	-139.0997252
C23-C21	1.5723706	C24-C23-C21	118.3461345	C25-C24-C23-C21	142.9297226
C24-C23	1.5343137	C25-C24-C23	120.9171161	C26-C24-C23-C21	-40.4877501
C25-C24	1.417941	C26-C24-C23	121.1192698	C27-C25-C24-C23	-179.2336638
C26-C24	1.4173825	C27-C25-C24	119.9271082	C28-C26-C24-C23	179.2298901
C27-C25	1.4000983	C28-C26-C24	119.955989	C29-C28-C26-C24	1.3055071
C28-C26	1.4002215	C29-C28-C26	122.4963789	C30-C23-C21-C20	92.6106398
C29-C28	1.3933835	C30-C23-C21	111.1111147	C31-C26-C24-C23	-1.9529269
C30-C23	1.5426542	C31-C26-C24	123.6898497	C32-C25-C24-C23	1.9150492
C31-C26	1.5177006	C32-C25-C24	123.6981816	C33-C29-C28-C26	178.9603817
C32-C25	1.5174733	C33-C29-C28	121.4346868	N34-C1-C20-C22	54.4028717
C33-C29	1.510343	N34-C1-C20	128.0588207	N35-C2-C1-N34	7.1718487
N34-C1	1.2859728	N35-C2-C1	68.7495542	O36-N34-C1-C20	0.2896802
N35-C2	1.2813086	O36-N34-C1	112.8969792	O37-N35-C2-C1	159.7114451
O36-N34	1.4094995	O37-N35-C2	112.9490519		
O37-N35	1.4102314				

Table 2. Theoretical and Experimental ^{1}H chemical shifts calculation for the title compound (ppm).

Atoms number	Theoretical calculation	Experimental calculation
H81	6.14	10.66-10.63
H79	5.93	10.66-10.63
H26	6.94	6.71
H58	6.94	6.71
H25	6.9	6.71
H59	6.89	6.71
H5	4.13	3.35-3.18
H15	4.05	2.52-2.31
H48	3.94	2.52-2.31
H17	3.93	2.52-2.31
H50	3.89	2.52-2.31
H8	3.35	3.35-3.18
H46	3.2	3.35-3.18
H9	2.97	3.35-3.18
H69	2.62	2.15
H18	2.62	3.35-3.18
H4	2.61	3.35-3.18
H66	2.58	2.15
H33	2.57	2.15
H36	2.57	2.15
H41	2.54	2.15
H74	2.54	2.15
H51	2.27	2.52-2.31
H16	2.21	2.52-2.31
H70	2.19	2.15
H14	2.17	2.52-2.31
H49	2.15	2.52-2.31
H65	2.13	2.15
H37	2.11	2.15
H32	2.09	2.15
H73	2.08	2.15
H42	2.06	2.15
H40	2.05	2.15
H75	2.04	2.15
H71	1.87	2.15
H34	1.87	2.15
H38	1.85	2.15
H67	1.83	2.15
H63	1.73	1.48
H28	1.65	1.48
H62	1.46	1.48
H30	1.43	1.48
H29	1.43	1.48
H61	1.43	1.48

The ^{1}H NMR chemical shifts for N-OH group theoretically equal to 6.03 (average), while experimentally equal to 10.64 (average). The aromatic protons' signals are well-known to occur at about 7 ppm. As a singlet peak chemical shift of H26, H58, H25, and H59 atoms was observed at 6.71 ppm. B3LYP/6-31G (d, p) methods discovered the average calculated ^{1}H NMR signals for these atoms at 6.91 ppm. The ^{1}H NMR chemical shift of (2x1H, cyclobutane; 2x2H, -CH_2-S) was observed at 3.26 ppm on average in the experimental spectrum, these chemical shifts were measured as 3.14 ppm on average for B3LYP/6-31G(d, p) levels. The CH_2- signals for cyclobutane rings occur at an average of 2.41 ppm, while this signal was computed at an average of 3.07 ppm for B3LYP/6-31G. (d, p). The experimentally chemical shift for CH_3-mesitylene and CH_3-cyclobutane equal to 2.15 and 1.48 ppm respectively. While the signals for those chemical shifts were computed equal to 1.95 and 1.69 ppm on average respectively.

Table 3. Theoretical and Experimental ^{1}H chemical shifts calculation for the title compound (ppm).

Atoms number	Theoretical calculation	Experimental calculation
C1	143.43	158.51
C2	142.85	158.51
C52	131.41	145.74
C19	130.91	145.74
C53	122.47	136.24
C21	122.24	136.24
C20	122.11	136.24
C54	122.05	136.24
C24	120.76	135.47
C57	120.37	135.47
C55	116.64	131.79
C23	116.62	131.79
C56	116.58	131.79
C22	116.53	131.79
C3	37.12	43.25
C47	36.8	41.82
C13	36.4	41.82
C7	35.22	43.25
C45	30.25	40.15
C12	29.53	40.15
C11	29.21	40.15
C44	29.03	40.15
C10	27.01	26.46
C43	25.89	26.46
C27	15.76	21.85
C60	15.5	21.85
C68	14.46	21.85
C35	14.44	21.85
C31	13.94	21.85
C64	13.93	21.85
C72	12.03	21.85
C39	11.94	21.85

In the ^{13}C NMR signals for C=N-OH was appeared at 158.51 experimentally, while theoretically appeared at 143.14 ppm. The signals at 145.74, 136.24, 135.47, and 131.79 ppm are assigned for Aromatic C's including (C52, C19), (C53, C21, C20, C54), (C24, C57), and (C55, C23, C56, C22), for those signals were calculated computed and found the average value at 131.16, 122.21, 120.56, and 116.59 ppm respectively. The cyclobutane, aliphatic-CH2, and CH3 carbons chemical shift were assigned at 43.25, 41.82, 40.15, 26.46, and 21.85 respectively, while for B3LYP/6-31G(d,p) methods, these signals were measured at 37.12, 36.6, 29.50, 26.45, and 14.00 ppm in average.

4.3 IR spectroscopy

IR spectrum was measured for the title compound both experimentally and theoretically. Using KBr pellets and a Mattson 1000 FT-IR spectrometer for experimentally IR spectrum and recorded in the range 4000–400 cm^{-1}. B3LYP/6-31G(d, p) methods were used to measure theoretical spectra. Both experimental and theoretical spectra are shown in Figure 3. The title compound has consisted of 81 atoms included hydrogen atoms and divided into two symmetry groups in the point of the sulfur atom. It has seen 237 natural modes of vibration. Table 3 lists several vibrational modes along with their experimental values.

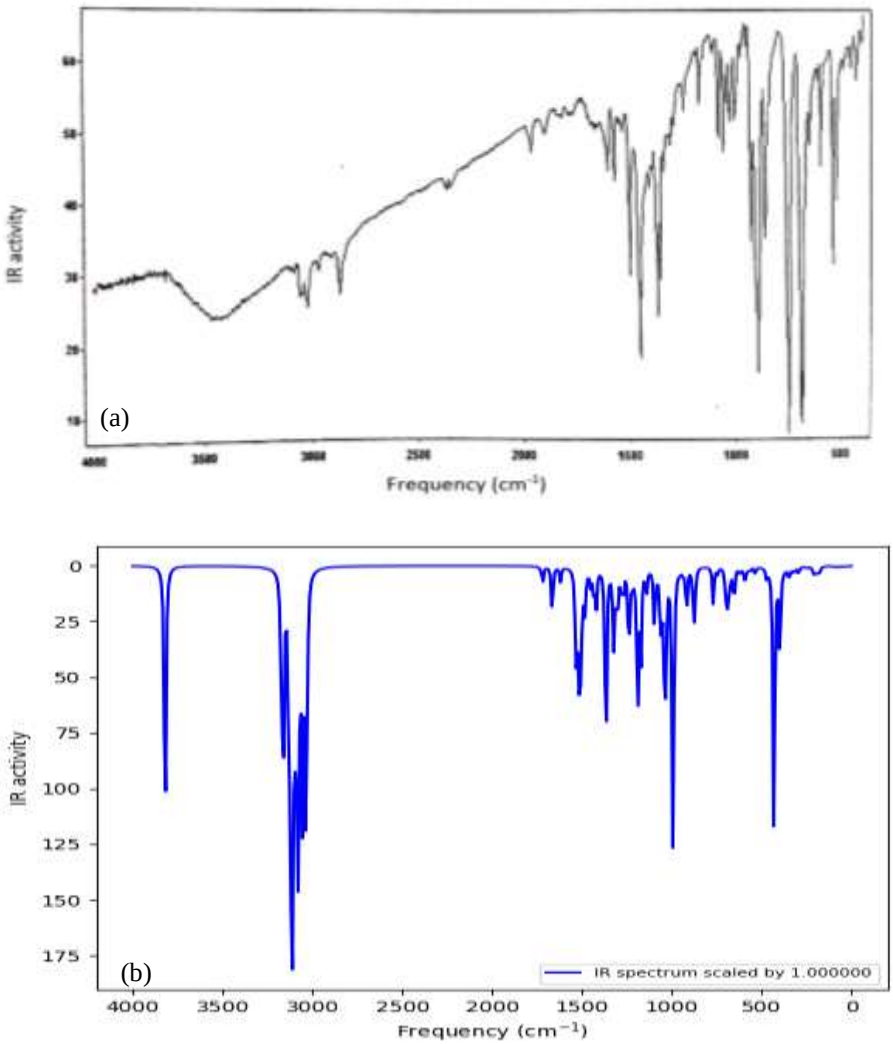

Figure 3. FT-IR spectra of the title compound at B3LYP/6-31G(d, p) levels. a) Experimental b) Theoretical results

Table 4. Comparison theoretical and experimental vibrational spectra of title compound (cm^{-1}).

Atoms Assignment	Theoretical Calculation	Experimental Calculation
N-OH, sv	3819.12	3348
N-OH, sv	3818.16	3253
C-H in CYB, sv	3176.19	
C-H in CYB, sv	3174	3165
CH2 in CYB, asv	3172.59	3107
CH2-S, asv	3166.35	
CH in MIS, sv	3160.56	3050
CH3 in MIS, asv	3132.26	
CH3 in CYB, asv	3116.18	
CH3 in MIS, asv	3113.01	
CH3 in CYB, asv	3093.35	
CH2 in CYB, sv	3078.22	
CH2-S, asv	3075.2	
CH in CYB, sv	3060.28	
CH3 in MSI, sv	3053.26	
CH2-S,sv	3051.63	2950
CH3 in CYB, sv	3038.43	2980
CH3 in CYB, sv	3038.18	2870
CH3 in MSI, sv	3034.19	
CH2-S, sv	3026.27	
C=N, sv	1735.06	1650
C=N, sv	1735.06	1600
C=C in MSI, sv	1664.67	1600
MSI group, sv	1618.7	
MSI group, sv	1617.94	
CH3 in MSI, asv	1533.26	
CH3 in MSI, asv	1532.84	
CH3 in CYB, asv	1518.86	
CH3 in MSI, asv	1517.16	
CH3 in MSI, asv	1507.93	
CH3 in CYB, asv	1504.46	
CH3 in MSI, asv	1504.14	
CH2 in CYB, sv	1485.82	
CH2-S, sv	1485.45	
CH2 in CYB, sv	1481.74	
CH3 in MSI, asv	1474.2	
C in MSI, sv	1451.57	
CH2-S, asv	1451.36	
C in MSI, sv	1451.16	
C-H in CYB, sv	1437.43	
C in MSI, sv	1321.38	
CH in MIS, sv	1288.74	
C in CYB, sv	1280.99	
CH2 in CYB, sv	1280.99	
CH2-S	1269.23	1260
CH2 CYB, sv	1257.78	
CH2 CYB, sv	1253.05	
C-C-N, asv	1221.43	1159
CH-S, asv	1208.26	
C in CYB, sv	1188.99	
C in MSI, asv	1096.03	
CH in MSI, ro,v	1063.08	
CH in MSI, si,v	1062.48	
CYB, asv	1036.16	
N-OH, sv	995.18	
C in Aromatic, sv	982.02	
C-H in MSI, ro,v	898.66	
C-C in CYB, sv	867.4	
C-S-C, sv	769.14	690
C-C in MSI, sv	759.97	
C-S-C, sv	671.41	655

Symmetrical: s, Vibration: v, unsymmetrical: a, Rocking: ro, scissoring: si, Mesitylene: MSI, cyclobutane: CYB

In aromatic compounds, the carbon-hydrogen stretching vibrations bands are signed in the range of 3100–3000 cm^{-1} [24-26]. The C-H asymmetric stretching was recorded at 3050 cm^{-1} in the FT-IR spectrum for the title molecule, which was also calculated as 3160.56 cm^{-1} B3LYP/6-31G(d, p) levels. The symmetric and asymmetric C-H_2 vibration mode known monitor of the cyclobutane ring was observed at 3107–2980 cm^{-1} range. In the FT-IR spectrum, C-H_2 stretches asymmetrically at 3107 cm^{-1}, this number is comparable in the literature [20, 27, 28]. In the FT-IR spectrum, symmetric stretching C-H_2 was observed at 2950 cm-1, and these vibrations were measured at 3051.63 for B3LYP/6-31G(d, p) levels. The C=N and C=C symmetric stretching vibrations have two bands at 1650 and 1600 cm^{-1}, respectively for FT-IR. While theoretically measured at 1735.06 for C=N and 1664.67 cm^{-1}. There are no major variations, as can be shown. The C-S-C stretching vibration has been allocated at range 690-655 cm^{-1} a very large band in the FT-IR. Both experimental and literature values agree well with the theoretically computed vibration frequency values.

We present correlation graphs based on the calculation in Figure 4 to compare with experimental observations. The correlation coefficient equals 0.9793, as can be seen from the correlation graphs.

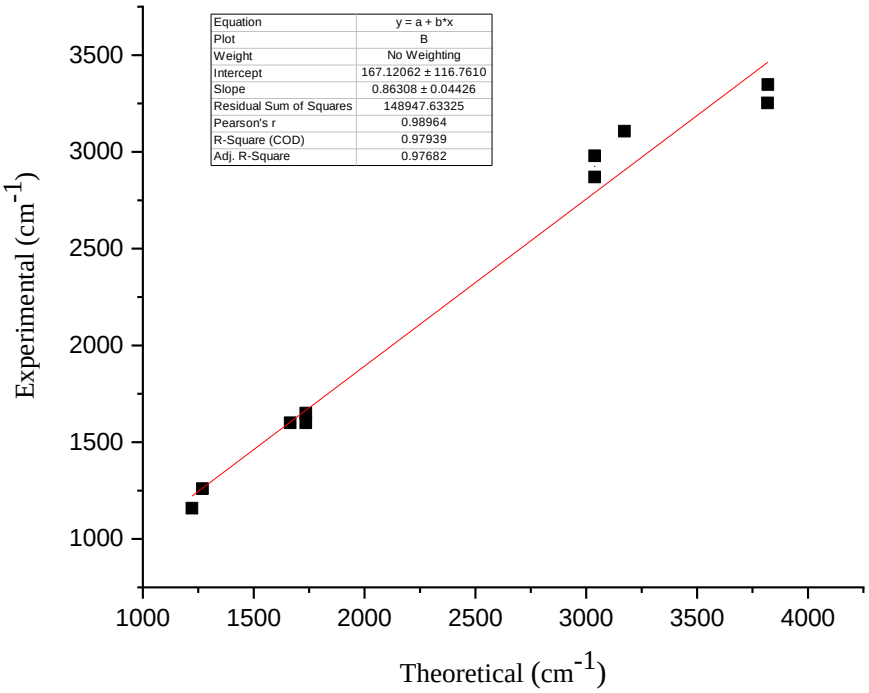

Figure 4. The experimental and theoretical vibration frequencies of the title compound are compared graphically (cm-1).

4.4 Study Inhibitor Activity

Identifier molecular structures which are related to electronic structure parameters including HOMO & LUMO energy level, energy bandgap (ΔE), χ, η, σ, ω, Pi, ε and μ. The HOMO, LUMO, and μ of the molecule are found from the output file in Gaussian, other parameters are calculated by existing equations. According to Koopman's theorem, the E_{HOMO} and E_{LUMO} values of any chemical form are correlated with their ionization energy and electron affinity values [29, 30]. The other parameters were calculated according to the following equations:

$$I = -E_{HOMO} \quad (1)$$

$$A = -E_{LUMO} \quad (2)$$

$$\Delta E = (E_{LUMO} - E_{HOMO}) \quad (3)$$

$$\eta = (I - A) / 2 \quad (4)$$

$$\sigma = 1/\eta \quad (5)$$

$$\chi = (I + A) / 2 \quad (6)$$

$$Pi = -\chi \quad (7)$$

$$\omega = Pi^2/2\eta \quad (8)$$

$$\varepsilon = Pi * \eta \quad (9)$$

Due to the overall electron flow between the transmitter and the receiver, the electrophilicity index (ω) is a measure of the energy depletion see equation (8). A new molecular structure identifier predictor in equation (9) is the nucleophilicity (ε) index. The following equation (ΔN) measures the number of electrons transferred between the inhibitor and the metal [31].

$$\Delta N = \frac{\chi metal - \chi inhibitor}{2.(\eta metal - \eta inhibitor)} \quad (10)$$

The χ and η inhibitor values in the equation are determined theoretically, while Pearson [32] experimentally calculates the χ metal and η metal values. according to Pearson as the electron affinity (A) and the ionization potential (I) of a single metal are assumed to be equal (I = A) and the η metal value for a single metal is assumed to be zero. The identifier's electronic structure parameters and total energy for title molecule were shown in Table 5.

Table 5. Quantum chemical parameters calculation for the title compound

Parameters	Equation	Results
Total Energy (a.u)		-1903.956
μ (D)		1.888
LUMO (eV)		-0.108
HOMO (eV)		-5.847
I (eV)	$I = -E_{HOMO}$	5.847
A (eV)	A = -ELUMO	0.108
ΔE (eV)	$\Delta E = (E_{LUMO} - E_{HOMO})$	5.738
η (eV)	$\eta = (I - A) / 2$	2.869
σ (eV)-	$\sigma = I/\eta$	2.037
χ (eV)	$\chi = (I + A) / 2$	2.978
Pi (eV)	$Pi = -\chi$	-2.978
ω (eV)	$\omega = Pi^2/\eta^2$	1.077
ε (eV)	$\varepsilon = Pi * \eta$	-8.546
ΔN	ΔN =(χmetal- χinhibitor)/2 (ηmetal- ηinhibitor)	0.875

When we look at the energies of HOMO and LUMO in Table 5 of the constructions tested, the HOMO and LUMO energy level for title compound equal to -5.847 and -0.108 eV respectively. Since HOMO is related to donating electrons capacity, it is essential for the studding of the corrosion. It can be seen

that as HOMO values increase, the inhibitory effect of inhibitor molecules increases [33]. Therefore, works on the mechanism of charge transfer along the metal surface, allowing adsorption. Based on the high E_{HOMO} value, our compound has higher inhibitory activity. LUMO is the ability to accept an electron. Low-value E_{LUMO} shows that the inhibitor will put an extra negative charge on the surface of the metal. The LUMO energy of our compound has the lowest energy. It was also observed that the LUMO energy values of inhibitors with high HOMO energy values inhibitor activity were high. The title compound has the most powerful corrosion inhibition, according to HOMO-LUMO capacity.

To evaluate the theoretical inhibition efficiency as well as static molecular reactivity, the energy gap between E_{HOMO} and E_{LUMO} has a very high preliminary significance and clarification. For inhibitor studies, it is appropriate to compare ΔE. The lower energy distances the increased efficiency of inhibition. In corrosion inhibitors, the lower value of ΔE relies on E_{HOMO} rather than E_{LUMO}. Inhibitor derivatives can be used as good anti-corrosion agents with high HOMO energy and low ΔE [33, 34]. It can be said that the title compound would have a strong inhibition activity depending on the highest HOMO energy value, provided the ΔE see Figure 5.

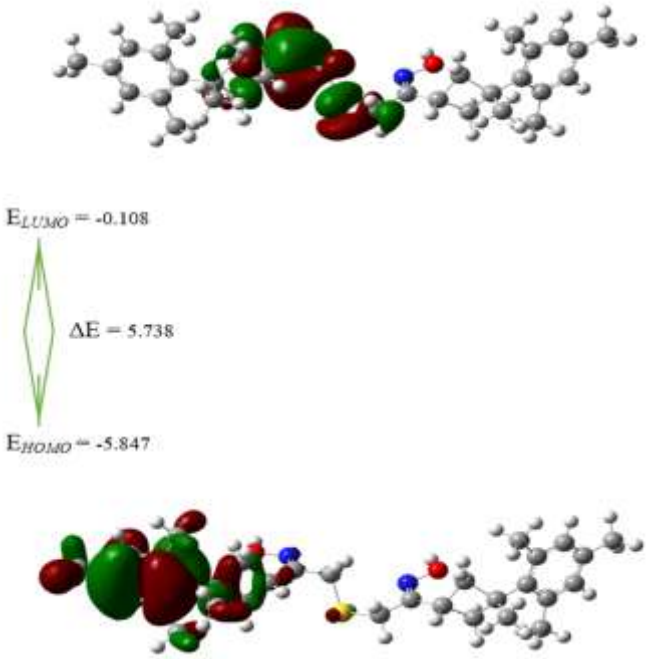

Figure 5. HOMO and LUMO energy level for title compound.

A common method for predicting the adsorption centers of the inhibitor molecules is the use of Mulliken population analysis [33]. Many researchers have advocated the existence of negatively charged heteroatoms to improve the ability to adsorb on the metal surface via the donor-acceptor process [35].

Due to the negatively charged nitrogen, oxygen, and carbon atoms in our title compound has more effective inhibitor activity. The charges of the atoms in our compound inhibitor's molecular structure are seen in Figure 6. It is seen the negative charge has more intensity on the atoms comparative with positive charge. This is representative of our title compound has good anti-corrosion activity.

Other significant parameters that provide information about an inhibitor's stability, reactivity, and inhibitor activity are η and σ. The η and σ for title compound are more close to each other see Table 5. Since the organic inhibitor chosen is lewis-based and soft inhibitors are more reactive than hard

inhibitors, they serve as stronger corrosion inhibitors [36]. Our compound inhibitors with high E_{HOMO} and low ΔE were estimated to have a high softness and low hardness values. The η and σ values support that the title compound has most powerful inhibitory activity.

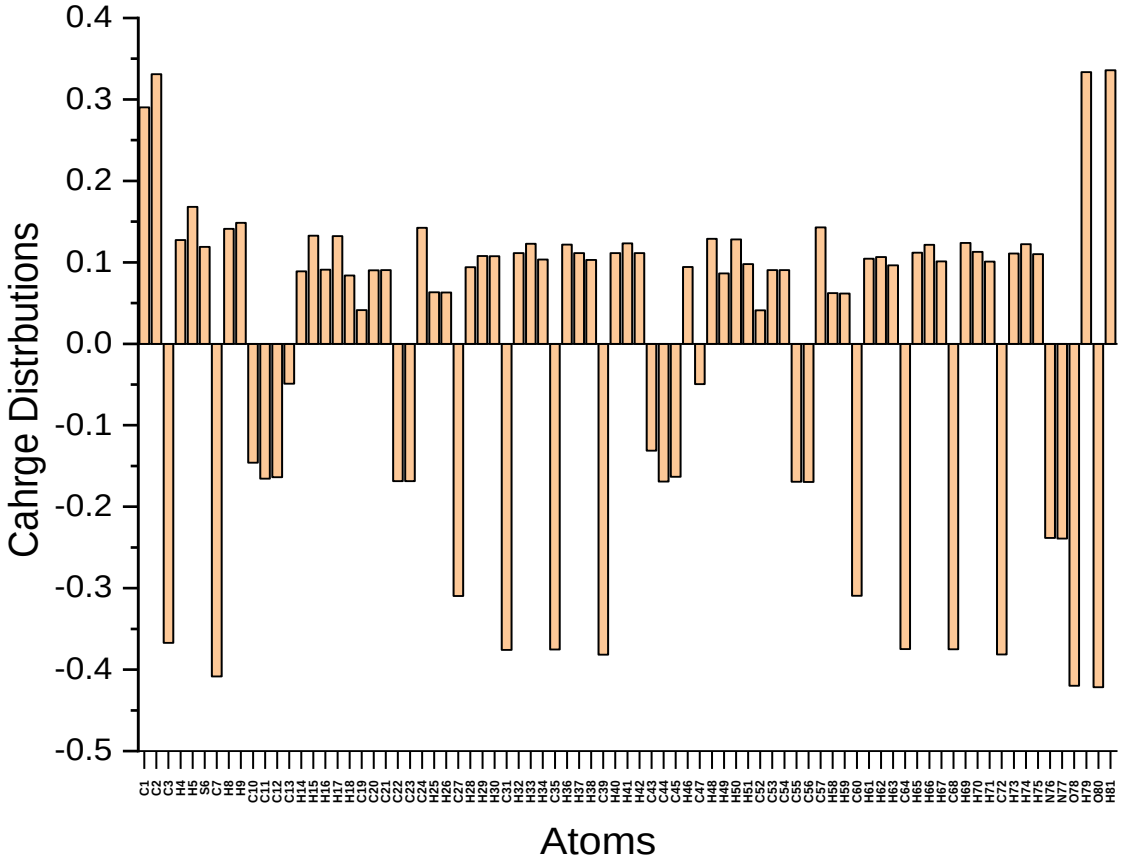

Figure 6. charge distribution on the atoms for title compound.

Further parameters that are measured for inhibitor activity are χ and Pi. Calculated inhibitor, χ values provide details about how the coordinated covalent bond happens between the metal and the inhibitor. In this report, the corrosion inhibition behavior of molecules intended as iron metal inhibitors were examined. It was found that the χ values of the inhibitors measured in Table 5 were smaller than the experimental χ value of the iron metal. The iron metal was form bonds by taking electrons from the inhibitor compound. The title compound inhibitor will serve as the most effective corrosion inhibitor with a higher χ value comparative with the literature [37, 38].

The dipole moment (μ) is another parameter illustrated in Table 5. However, literature studies have not found a direct correlation between μ and the activity of inhibition. In some studies, the activity of molecules with a higher μ value is to be better inhibition whereas, in other studies, the inhibition effect is increased with a decreased μ value. The μ for title compound was equal to 1.888 D [31, 33, 34].

The ω and ε are important parameters used to determine inhibitors to corrosion activities. The ω shows the inhibitor molecules' ability to accept electrons and ε shows inhibitors molecule ability to donate electrons. The activity of inhibition increases as the ε value increases and the ω value decreases [39, 40]. In our molecule, the ε increase and ω have decreased. It is noted that, according to ω and ε parameters, our compound has the most powerful inhibitor activity. According to ΔN [34] results, the

title compound has a good inhibitor, which means more electron transfer from organic compound the surface of iron metals.

5. Conclusion

The title compound was successfully synthesized and spectroscopy characterization for both experimental and theoretically were good arguments to each other. The beginning geometry was achieved using the Density Functional Theory (DFT)/B3LYP form, with basis sets of 6-31G(d, p). According to the results obtained, our compound has E_{HOMO} values for inhibitors are high and E_{LUMO} values were found in lower. For this resin, it was determined donor compound and had high inhibitor activity. As good anti-corrosion agents, inhibitor derivatives with high E_{HOMO} and low ΔE can be used. It can be said that strong inhibition activity depending on the highest value of E_{HOMO} and lower ΔE. Viewed as suggesting that our compound used in the study is better at hiding the metal surface at a low dipole moment value, although the literature does not find a strong conclusion about the dipole moment. When you look at the atomic charges of the compound inhibitor it is said that the electronegative atoms have a major influence on the action of inhibition. The most active area shown in the oxygen(s) and Nitrogen(s). The determined parameters of η, ω, σ, ε, Pi and χ support that the title compound has most powerful inhibitor effect corrosion inhibition. The inhibitor's lower χ value means that the iron metal can form a bond by taking electrons from the compound inhibitor. The higher value ΔN of the inhibitor indicates that the metal surface will be better adsorbed and the effect of corrosion inhibition will increase.

Author(s) Contributions

Each author's contribution to the study is 25%.

Conflicts of Interest

There are no conflicts to declare.

References

[1]. Chakravorty A., "Structural chemistry of transition metal complexes of oximes", Coordination Chemistry Reviews, 1974, 13(1): 1-46.
[2]. Pavia D. L., Lampman G. M., Kriz G. S. and Vyvyan J., "Introduction to Spectroscopy, Brooks", Cole, Cengage Learning, 2009.
[3]. Karipcin F. and Arabali F., "Synthesis and characterization of 4-arylaminobiphenylglyoximes and their complexes", Journal of the Chilean Chemical Society, 2006, 51(3): 982-985.
[4]. Al-Sha'alan N. H., "Antimicrobial activity and spectral, magnetic and thermal studies of some transition metal complexes of a Schiff base hydrazone containing a quinoline moiety", Molecules, 2007, 12(5): 1080-1091.
[5]. Yaul S. R., Yaul A., Pethe G. B. and Aswar A. S., "Synthesis and characterization of transition metal complexes with N, O-chelating hydrazone Schiff base ligand", Am-Euras. J. Sci. Res, 2009, 4(4): 229-234.
[6]. Demir I., Bayrakcı M., Mutlu K. and Pekacar A. I., "Synthesis and Characterization of a Novel Iminooxime Schiff Base Ligand and Its Complexation with Copper (II), Nickel (II), Zinc (II), Cadmium (II), and Cobalt (II)", Acta Chimica Slovenica, 2008, 55(1).

[7]. Bailey S. E., Olin T. J., Bricka R. M. and Adrian D. D., "A review of potentially low-cost sorbents for heavy metals", Water research, 1999, 33(11): 2469-2479.
[8]. Babahan I., Coban E. P. and Biyik H., "Synthesis, characterisation and antimicrobial activities of vic-dioxime derivatives containing heteroaromatic hydrazone groups and their metal complexes", Maejo International Journal of Science and Technology, 2013, 7(1): 26-41.
[9]. Topal T., Kart H. H., Taşlı P. T. and Karapınar E., "Synthesis and structural study on (1E, 2E, 1′ E, 2′ E)-3, 3′-bis [(4-bromophenyl)-3, 3′-(4-methy-1, 2-phenylene diimine)] acetaldehyde dioxime: A combined experimental and theoretical study", Optics and Spectroscopy, 2015, 118(6): 865-881.
[10]. Chitrapriya N., Mahalingam V., Zeller M., Lee H. and Natarajan K., "Synthesis, characterization, DNA binding and cleavage studies of Ru (II) complexes containing oxime ligands", Journal of Molecular Structure, 2010, 984(1-3): 30-38.
[11]. Ganguly S., Karmakar S., Pal C. K. and Chakravorty A., "Regiospecific oximato coordination at the oxygen site: ligand design and low-spin MnII and FeII/III species", Inorganic chemistry, 1999, 38(26): 5984-5987.
[12]. AHMED L. and Rebaz O., "Spectroscopic properties of Vitamin C: A theoretical work", Cumhuriyet Science Journal, 41(4): 916-928.
[13]. Miehlich B., Savin A., Stoll H. and Preuss H., "Results obtained with the correlation energy density functionals of Becke and Lee, Yang and Parr", Chemical Physics Letters, 1989, 157(3): 200-206.
[14]. Antony J. and Grimme S., "Density functional theory including dispersion corrections for intermolecular interactions in a large benchmark set of biologically relevant molecules", Physical Chemistry Chemical Physics, 2006, 8(45): 5287-5293.
[15]. Omer R. A., Ahmed L. O., Koparir M. and Koparir P., "Theoretical analysis of the reactivity of chloroquine and hydroxychloroquine", Indian Journal of Chemistry-Section A (IJCA), 2020, 59(12): 1828-1834.
[16]. Gaussian09 R. A., "1, mj frisch, gw trucks, hb schlegel, ge scuseria, ma robb, jr cheeseman, g. Scalmani, v. Barone, b. Mennucci, ga petersson et al., gaussian", Inc., Wallingford CT, 2009, 121: 150-166.
[17]. Dennington R., Keith T. and Millam J. G., "Version 4.1. 2", Semichem Inc, 2007.
[18]. Şen F., Dinçer M., Çukurovalı A. and Yılmaz İ., "(Z)-1-(3-Mesityl-3-methylcyclobutyl)-2-(morpholin-4-yl) ethanone oxime", Acta Crystallographica Section E: Structure Reports Online, 2011, 67(4): o958-o959.
[19]. Şen F., Dinçer M., Çukurovalı A. and Yılmaz I., "1, 1′-Bis (3-methyl-3-phenylcyclobutyl)-2, 2′-(azanediyl) diethanol", Acta Crystallographica Section E: Structure Reports Online, 2012, 68(4): o1052-o1052.
[20]. Şen F., Dinçer M. and Cukurovali A., "Synthesis, spectroscopic characterization and quantum chemical computational studies on 4-(3-methyl-3-phenylcyclobutyl)-2-(2-undecylidenehydrazinyl) thiazole", Journal of Molecular Structure, 2014, 1076: 1-9.
[21]. Şen F., Ekici Ö., Dinçer M. and Cukurovali A., "A comparative study on 4-(4-(3-mesityl-3-methylcyclobutyl) thiazole-2-yl)-1-thia-4-azaspiro [4.5] decan-3-one: Experimental and density functional methods", Journal of Molecular Structure, 2015, 1086: 109-117.
[22]. Jian F. F., Zhao P. S., Bai Z. S. and Zhang L., "Quantum chemical calculation studies on 4-phenyl-1-(propan-2-ylidene) thiosemicarbazide", Structural Chemistry, 2005, 16(6): 635-639.
[23]. Allen F. H., "The geometry of small rings. VI. Geometry and bonding in cyclobutane and cyclobutene", Acta Crystallographica Section B: Structural Science, 1984, 40(1): 64-72.
[24]. Cansiz A., Etin A., Kutulay P. and Koparir M., "Synthesis of Tautomeric Forms of 5-(2-Hydroxyphenyl)-4-substituted-3H-1, 2, 4-triazole-3-thione", Asian Journal of Chemistry, 2009, 21(1): 617.

[25]. Arslan N. B., Özdemir N., Dayan O., Dege N., Koparır M., Koparır P. and Muğlu H., "Direct and solvent-assisted thione–thiol tautomerism in 5-(thiophen-2-yl)-1, 3, 4-oxadiazole-2 (3H)-thione: Experimental and molecular modeling study", Chemical Physics, 2014, 439: 1-11.
[26]. Koparir P., Sarac K., Orek C. and Koparir M., "Molecular structure, spectroscopic properties and quantum chemical calculations of 8-t-buthyl-4-methyl-2H-chromen-2-one", Journal of Molecular Structure, 2016, 1123: 407-415.
[27]. İnkaya E., Dinçer M., Ekici Ö. and Cukurovali A., "N′-(2-methoxy-benzylidene)-N-[4-(3-methyl-3-phenyl-cyclobutyl)-thiazol-2-yl]-chloro-acetic hydrazide: X-ray structure, spectroscopic characterization and DFT studies", Journal of Molecular Structure, 2012, 1026: 117-126.
[28]. Rebaz O., KOPARIR P., AHMED L. and KOPARIR M., "Computational determination the reactivity of salbutamol and propranolol drugs", Turkish Computational and Theoretical Chemistry, 4(2): 67-75.
[29]. Koopmans T., "Über die Zuordnung von Wellenfunktionen und Eigenwerten zu den einzelnen Elektronen eines Atoms", Physica, 1934, 1(1-6): 104-113.
[30]. Plakhutin B. N. and Davidson E. R., "Koopmans' Theorem in the Restricted Open-Shell Hartree−Fock Method. 1. A Variational Approach", The Journal of Physical Chemistry A, 2009, 113(45): 12386-12395.
[31]. Musa A. Y., Jalgham R. T. and Mohamad A. B., "Molecular dynamic and quantum chemical calculations for phthalazine derivatives as corrosion inhibitors of mild steel in 1 M HCl", Corrosion Science, 2012, 56: 176-183.
[32]. Pearson R. G., "Absolute electronegativity and hardness: application to inorganic chemistry", Inorganic chemistry, 1988, 27(4): 734-740.
[33]. Chen S., He B., Liu Y., Wang Y. and Zhu J., "Quantum chemical study of some benzimidazole and its derivatives as corrosion ınhibitors of steel in HCl solution", Int. J. Electrochem. Sci, 2014, 9: 5400-5408.
[34]. Beytur M., Irak Z. T., Manap S. and Yüksek H., "Synthesis, characterization and theoretical determination of corrosion inhibitor activities of some new 4, 5-dihydro-1H-1, 2, 4-Triazol-5-one derivatives", Heliyon, 2019, 5(6): e01809.
[35]. El Adnani Z., Mcharfi M., Sfaira M., Benzakour M., Benjelloun A. and Touhami M. E., "DFT theoretical study of 7-R-3methylquinoxalin-2 (1H)-thiones (RH; CH3; Cl) as corrosion inhibitors in hydrochloric acid", Corrosion Science, 2013, 68: 223-230.
[36]. Alexander D. and Moccari A., "Evaluation of corrosion inhibitors for component cooling water systems", Corrosion, 1993, 49(11): 921-928.
[37]. Martinez S., "Inhibitory mechanism of mimosa tannin using molecular modeling and substitutional adsorption isotherms", Materials chemistry and physics, 2003, 77(1): 97-102.
[38]. Issa R. M., Awad M. K. and Atlam F. M., "Quantum chemical studies on the inhibition of corrosion of copper surface by substituted uracils", Applied Surface Science, 2008, 255(5): 2433-2441.
[39]. Karakus N. and Sayin K., "The investigation of corrosion inhibition efficiency on some benzaldehyde thiosemicarbazones and their thiole tautomers: Computational study", Journal of the Taiwan Institute of Chemical Engineers, 2015, 48: 95-102.
[40]. Kariper S. E., Sayın K. and Karakaş D., "Theoretical studies on eight oxovanadium (IV) complexes with salicylaldehyde and aniline ligands", Hacet. J. Biol. Chem., 2014, 42(3): 337-342.